

Research papers

Modified sodium acetate trihydrate/expanded perlite composite phase change material encapsulated by epoxy resin for radiant floor heating

Henghua Zhang^a, Qianbin Dong^a, Juetian Lu^a, Yaping Tang^b, Wenjian Bi^b, Yue Gao^b, Hui Yang^{a,c}, Jiabang Wang^{a,*}

^a School of Materials Science and Engineering, Zhejiang University, Hangzhou 310027, PR China

^b Zhejiang Kesheng Technology Co., LTD, Hangzhou 310027, PR China

^c Zhejiang California International Nano Systems Institute, Hangzhou 310027, PR China



ARTICLE INFO

Keywords:

Composite phase change material
Epoxy resin
Coating encapsulated phase change material
Phase change radiant heating system

ABSTRACT

In this study, sodium acetate trihydrate was modified with urea, ethylene glycol, and disodium hydrogen phosphate dodecahydrate. The modified phase change material was impregnated into expanded perlite to obtain a composite phase change material, which was encapsulated with epoxy resin as the coating to obtain a coated composite phase change material with a phase change temperature of 46.4 °C, a latent heat of phase change of 132.7 J/g, and a low supercooling temperature of 0.6 °C. Leak tests and thermal cycle stability showed that the coating could effectively slow down the escape rate of the liquid phase and solve the macroscopic leakage problem. Moreover, the decrease in latent heat was only 1.8 % after 100 cycles, demonstrating excellent thermal cycle stability. The morphology and elemental distribution of the modified phase change materials and coatings were studied. In addition, laboratory insulation simulation tests were conducted, and the coated composite phase change material panels showed a significant delay in temperature reduction, while the insulation box showed longer lasting thermal performance. The excellent properties of the material find their application in radiant floor heating systems and play a key role in the expansion of coated phase change materials.

1. Introduction

Nowadays, with the rapid growth of the population, global energy consumption is expected to continuously grow [1]. The demand for energy consumption in the building sector accounts for about 40 % of its total consumption [2]. Therefore, it is important to conserve and use energy effectively. Radiant floor heating [3] is a heating method that evenly dissipates heat into the room by means of heat radiation and heat convection through the ground. It is widely used in domestic and commercial buildings due to its ability to provide comfortable indoor temperatures, effective use of building space, and rational use of low-grade energy. In particular, the use of phase change latent heat storage technology for radiant floor heating systems can reasonably balance the energy supply demand [4]. The use of phase change latent heat storage technology in radiant floor heating systems can balance the demand for energy supply, such as storing electrical energy as heat during off-peak periods and releasing it when needed during peak periods, thus achieving more efficient use of energy [5,6].

Compared to sensible heat storage materials, phase change materials

have the advantages of higher latent heat of phase change, constant phase change temperature, smaller phase change volume change, etc. They can be categorized into organic and inorganic materials according to their chemical composition. The organic phase change materials represented by paraffin wax [7], fatty acids [8], and aliphatic alcohols [9] do not undergo supercooling during the phase change process while having very excellent chemical stability and exhibiting small changes in latent heat of phase change after multiple heat storage and release cycle [10], garnering attention from researchers. However, the high cost, flammability, and irritating odour of organic phase change materials limit their practical applications [11]. Inorganic phase change materials, especially hydrated salts, show the advantage of having an adjustable phase change temperature and non-flammability [10]. Inorganic hydrated salt phase change materials have excellent thermal energy storage capacity and have shown great potential in the construction field [12]. However, inorganic phase change materials are prone to leakage during the solid-liquid phase transition, have high supercooling temperatures, and lose crystalline water in the air easily during the phase change process [13,14], severely affecting their actual service life.

Currently, the most common solution to the liquid leakage problem

* Corresponding author.

E-mail address: msewjbang@zju.edu.cn (J. Wang).

Abbreviations

PCM	Phase Change Material
SAT	Sodium Acetate Trihydrate
EG	Ethylene Glycol
DSP	Disodium hydrogen phosphate dodecahydrate
EP	Expanded Perlite
ER	Epoxy Resin
MPCM	Modified Phase Change Material
CPCM	Composite Phase Change Material
Coated, CPCM	Coated Composite Phase Change Material
ΔH	enthalpy change, J/g
m	the mass of the sample, g
T	temperature, °C

caused by the solid-liquid transition that occurs during the phase change process is to use high porosity water absorbent composite materials with a high specific surface area such as porous carbon [15,16], porous mineral-based [17,18], and polymeric materials [19,20]. Such materials can store the liquid in their porous structures and restrict the flow of liquids, thus are cheap and easy to use [21]. Among all, expanded perlite is a porous mineral-based material with a high specific surface area, high adsorption capacity, light-weight, and good refractoriness, which is widely used in the field of building energy efficiency. There have been several studies on the combination of expanded perlite with phase change materials to prevent liquid phase leakages, such as the combination of expanded perlite with organic phase change materials and the material used in cement mortar [22]; whereas the combination of expanded perlite with inorganic hydrated salt phase change material has been made into phase change material insulation board for wall insulation [23,24]. Among them, Huang [25] prepared a new SFMS/EP composite phase change material by combining SFMS, a mixture of 77.6 wt% sodium acetate trihydrate and 19.4 wt% formamide, with expanded perlite. The SFMS/EP material containing 55 % SFMS showed a 4.25 % decrease in latent heat after multiple cold and thermal cycle tests.

Solving the aforementioned problem becomes a prerequisite for the efficient use of phase change materials in the long term. In micro-encapsulated phase change material having the phase change material as the core and an organic polymer as the shell [26,27], the microencapsulation technique is a potential method to solve the leakage problem. Peng et al. [28], prepared a microencapsulated phase change material with n-tetradecane and m-xylene as the core and epoxy resin as the capsule. The synthesized material showed a latent heat that can be flexibly adjusted in the range of 32.41–50.75 J/g. Owing to the protective effect of the epoxy resin, the composite phase change material was able to maintain stable performance below 300 °C, and the latent heat did not change significantly after cycling. Wang [29] prepared microencapsulated materials (CS-MCPMC) with melamine-formaldehyde resin as the shell and octadecyl methacrylate and n-octadecane as the phase change materials by in-situ polymerization, and the results showed that the CS30%-MCPMCs had no macroscopic leakage after 150 cycles and exhibited very excellent thermal cycling stability. Based on the adsorption of expanded perlite and the combination of the fixed and microencapsulated phase change materials, the application of the organic coating on the surface of expanded perlite is expected to avoid direct exposure of the phase change materials to air, thereby preventing moisture evaporation and liquid phase leakage. Similar studies, such as the double encapsulation of paraffin by porous graphite foam and epoxy resin [30], polymer coated with $\text{CaCl}_2 \cdot 6\text{H}_2\text{O}$ /EG composites [31], and encapsulation of $\text{Na}_2\text{CO}_3 \cdot 10\text{H}_2\text{O}$ - $\text{Na}_2\text{HPO}_4 \cdot 12\text{H}_2\text{O}$ /diatomaceous earth by UV-curable urethane acrylate [32], had achieved the expected results.

Most of the previous studies on the preparation of composite phase change materials using expanded perlite as a carrier only stayed at the adsorption stage, that is to say, only how to solve the formation of phase change materials was considered. However, there are few kinds of researches on coating epoxy resin on PCM to further alleviate the liquid phase leakage problem and improve the high storage-release efficiency of composite materials during the cycle. The innovation of this paper is inspired by the micro-encapsulated phase change material with a cyst-shell structure. Based on the expanded perlite as the carrier, the expanded perlite/phase change material is coated with epoxy resin, which can effectively relieve the liquid phase leakage and slow down the volatilization of crystal water in the phase change material to a certain extent, and ensure the energy storage density and heat release time of the material in the recycling process.

In this study, sodium acetate trihydrate was selected as the main phase change material, considering that the working temperature of the actual phase change radiation plate ranges between 40 and 50 °C and the phase change temperature of sodium acetate trihydrate is about 58 °C. A certain proportion of urea and ethylene glycol were introduced simultaneously to adjust the phase change temperature of sodium acetate trihydrate to obtain the modified phase change material (MPCM). Expanded perlite was chosen as the adsorption support to obtain the composite phase change material (CPCM) by vacuum adsorption method. Epoxy resin was selected as the coating material due to its excellent thermal stability, durable chemical resistance, and dense three-dimensional network structure formed after curing with a curing agent. Coated CPCM was obtained by coating the resin on CPCM. This study aimed to obtain a modified sodium acetate trihydrate/expanded perlite composite phase change material encapsulated by epoxy resin, whose coating encapsulation effect, phase change behaviour, and stability of Coated CPCM after thermal cycling were investigated. The results showed that the composite phase change material encapsulated by epoxy resin experienced almost no latent heat loss after thermal cycling exhibited excellent thermal reliability, and could be used for a longer time, improving its efficiency.

2. Experiments

2.1. Materials

Table 1 lists the product information for selected reagents.

Expanded perlite (EP): particle size about 1.25–1.60 mm, purchased from China Xinyang Zhongkai Insulation Material Co. Waterborne epoxy resin (ER), epoxy equivalent 180–190 g/Eg, waterborne epoxy curing agent, amine value 230 ± 30 mg KOH/g, average solid content about 60 %, purchased from Shenzhen Jitian Chemical Co.

2.2. Preparation of CPCM

For MPCM solution preparation, a mixture of 10.00 g SAT, 0.50 g Urea, and 0.40 g EG was placed in a beaker and heated in a water bath at 60 °C for 30 min until complete dissolution. Then, 0.15 g of nucleating agent DSP was added and the solution was stirred magnetically at a rate of 400 rpm for 30 min at 60 °C to form a homogeneous MPCM solution.

Table 1
Product information for selected reagents.

Sample name	Purity	Manufacturer
Sodium acetate trihydrate (SAT)	AR, 99.0 %	Shanghai Aladdin Biochemical Technology Co.
Urea	AR, ≥ 99.5 %	Shanghai Aladdin Biochemical Technology Co.
Ethylene glycol (EG)	AR, 98.0 %	Shanghai Aladdin Biochemical Technology Co.
Disodium hydrogen phosphate dodecahydrate (DSP)	AR, ≥ 99.0 %	Sinopharm Chemical Reagent Co.

The MPCM was prepared by vacuum impregnation method. For CPCM, prior to the impregnation phase, expanded perlite of suitable particle size was screened using sieves with apertures of 1.25 mm and 1.60 mm and dried in an oven at 105 °C for 24 h to remove moisture. The pre-treated EP was added to the MPCM in proportion (MPCM was 70 wt %, 75 wt%, 80 wt%, and 85 wt% of the total mass), sealed in a container after thorough stirring, and placed in a vacuum oven at 60 °C and 0.08 MPa for 30 min. This process was repeated three times to ensure that the MPCM was fully adsorbed by the EP to obtain CPCM.

2.3. Preparation of coated CPCM

In order to study the specific amount of epoxy resin used, the present experiment was carried out according to the optimum adsorption ratio of epoxy resin (with hardener) to expanded perlite mass i.e., ER: EP = 0.4, 0.6, 0.8, 1.0, 1.2 and above for the encapsulation. The predetermined amount of epoxy resin and hardener were added to the beaker separately, mixed and stirred, and later mixed with CPCM. The sample, after sufficient mixing, was left to cure at room temperature for 24 h. Eventually, the Coated CPCM was obtained. Fig. 1 shows the preparation process of Coated CPCM.

2.4. Characterization

The samples were observed for microscopic morphology and structure using a scanning electron microscope (SEM, SU-3500, Hitachi, Japan). The samples were subjected to 120 s of gold sputter coating, an acceleration voltage of 5 kV, and a scanning voltage of 10 KV for EDS.

The phase change temperature and the latent heat of phase change of the samples were tested using a differential scanning calorimeter (DSC, TA Q200, Instruments, USA) in the range 0–80 °C at a heating rate of 5 °C/min under N₂ atmosphere with a measurement accuracy of ±0.01 °C. The phase change temperature was determined from the intersection of the extrapolation line at the maximum slope of the DSC curve peak with the baseline, and the latent heat of phase change was determined from the integral of the peak area.

Data on the heat absorption-dissipation behaviour and on the magnitude of supercooling during heating and cooling of the samples were recorded and collected every 10 s, using a temperature logger with a thermocouple (SSN61, YOWEXA, China) placed at a fixed position. The measurement accuracy was ±0.5 °C. Thermal decomposition

analysis was performed using a thermogravimetric analyser with a test range of 25–600 °C at a heating rate of 10 °C/min under N₂ atmosphere.

The chemical composition of the sample was analysed using Fourier infrared spectroscopy (FT-IR, Nicolet iS20, Thermo Scientific, USA), where the sample under test was ground and pelletised with a certain amount of KBr, using a scanning range of 450–4000 cm⁻¹ and a resolution of 4 cm⁻¹. X-ray diffractometer (XRD, Rigaku Ultima IV, Rigaku, Japan) was used to analyse the phase of the sample. The test range was 10°–80°, and the sample was scanned at a scanning speed of 5°/min. X-ray photoelectron spectrometer (XPS, K-Alpha, Thermo Fisher Scientific, USA) was used to analyse the coordination states of the elements in the samples. Automatic mercury injection instrument (AutoPore IV 9500, Micromeritics, USA) was used to test the pore distribution characteristics and surface area distribution of different samples.

The thermal cycling stability of the CPCM and Coated CPCM were assessed by a water bath heating (60 °C)–air cooling (20 °C) process over 100 cycles, with all tests repeated three times.

3. Results and discussion

3.1. Effect of different contents of urea and ethylene glycol on SAT phase change temperature

Generally speaking, the application of ideal phase change materials has the requirements of suitable phase change temperature and high energy storage density. In this study, it was found that urea alone was used to adjust the phase change temperature of SAT, and the phenomenon of latent heat decreased significantly after reaching a certain amount, which was not conducive to the requirement of high energy storage density of phase change materials. Therefore, urea and ethylene glycol are selected to jointly adjust the phase change temperature of SAT. First, the temperature regulation effect of urea was explored, and the DSC curve of 1–9 wt% urea addition was studied, as shown in Fig. 2 (a), and the relevant thermophysical parameters are listed in Table 2. The criterion for temperature regulation of phase change materials is to keep the latent heat as high as possible under the condition that the material reaches a suitable phase change temperature. Therefore, comparing the data in Table 2, the urea content of 5.0 wt% is selected as the optimal content, because the phase change temperature of 52.6 °C at 5.0 wt% is lower than the temperature of 51.3 °C at 7.0 wt%, but the latent heat decreased significantly. Therefore, considering that the

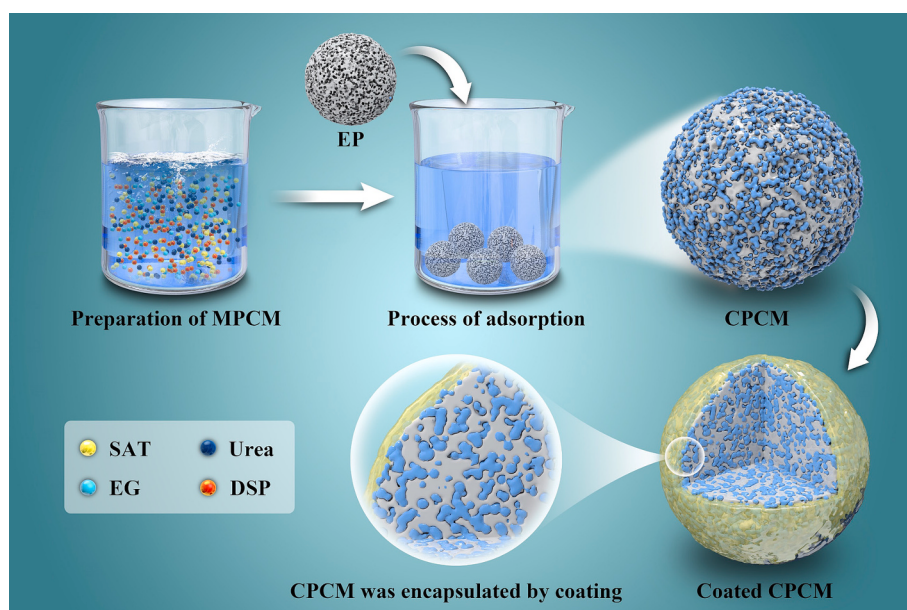


Fig. 1. Flow chart of the preparation of Coated CPCM.

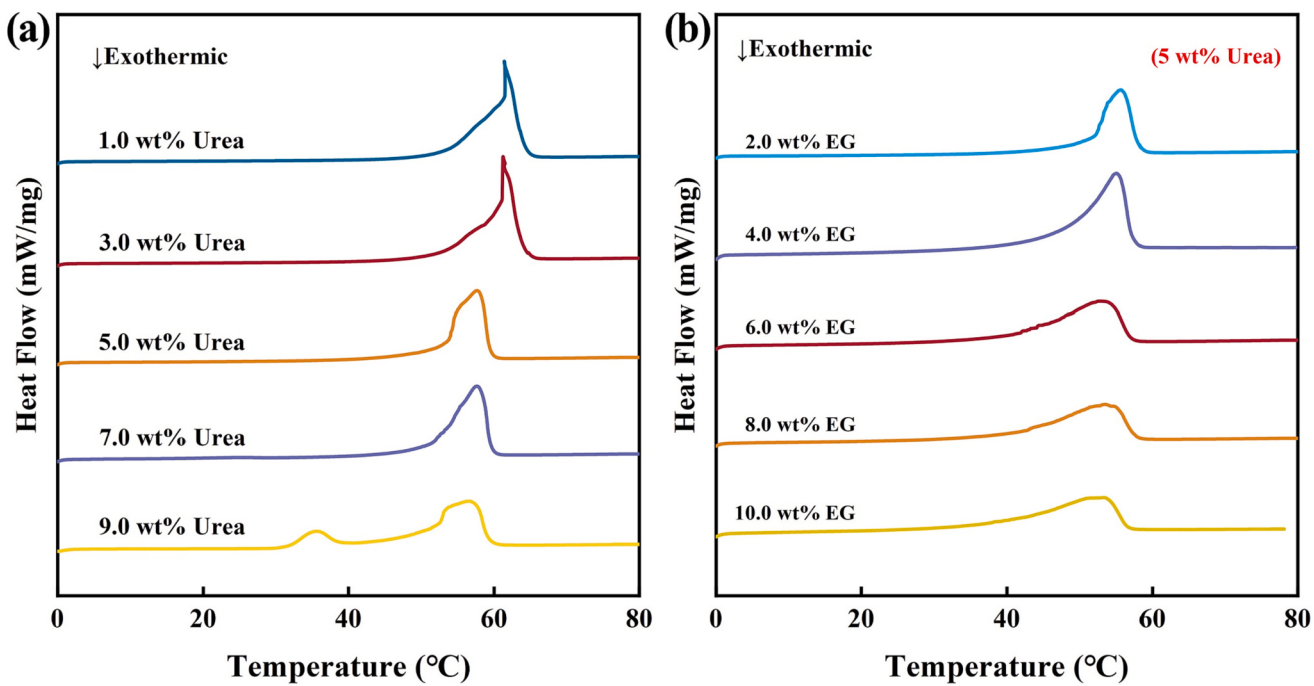


Fig. 2. (a) DSC curves of $\text{CH}_3\text{COONa}\cdot 3\text{H}_2\text{O}$ under different urea additions, (b) DSC curves of $\text{CH}_3\text{COONa}\cdot 3\text{H}_2\text{O}$ under different ethylene glycol additions (Pre-add 5.0 wt% Urea).

Table 2

Thermophysical parameters of phase change materials with different contents of urea and ethylene glycol.

Additive	Urea					EG (5 wt% Urea)				
Content (wt%)	1.0	3.0	5.0	7.0	9.0	2.0	4.0	6.0	8.0	10.0
ΔH (J/g)	265.7	259.4	254.2	242.4	221.9	249.6	244.5	234.3	223.6	181.4
T (°C)	57.6	56.5	52.6	51.3	51.6	50.7	49.1	47.4	44.1	38.0

material should try to meet the high energy storage density within a certain temperature range, the addition amount of 5.0 wt% was selected as the optimal addition amount. The phase change temperature of 52.6 °C with 5.0 wt% urea was still higher than the comfortable temperature of floor radiation, so ethylene glycol was selected to continue temperature adjustment on this basis. By comparing the data in Table 2, it can be seen that the phase change temperatures of materials with the addition of 4.0 wt%, 6.0 wt%, and 8.0 wt% glycol are 49.1 °C, 47.4 °C, and 44.1 °C respectively, which meet the temperature range of floor radiant heating. However, the addition of 4.0 wt% maintains the highest

latent heat of phase change of 240.7 J/g among the three. Therefore, ethylene glycol content of 4.0 wt% was selected as the optimal addition amount.

3.2. Study on optimal content of urea and ethylene glycol

In this study, the post-vacuum adsorption condition is utilised to determine the optimum amount of expanded perlite to be added, i.e., it is explored by observing and calculating the amount of MPCM remaining on the vessel wall. Fig. 3(a) shows the physical graphs before and

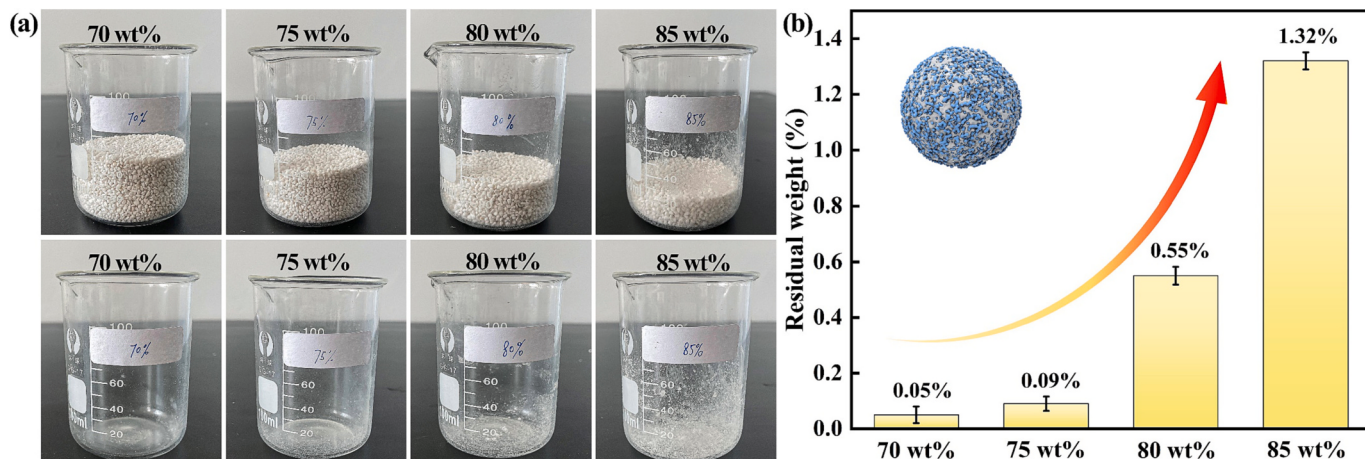


Fig. 3. (a) Physical diagram of MPCM adsorbed with different mass percentages, (b) Residual weight at different mass fractions.

after the adsorption of MPCM at 70 wt%, 75 wt%, 80 wt%, and 85 wt%, and it can be seen that the residual MPCM on the beaker gradually increases as the MPCM mass fraction increases. When MPCM was at 80 wt % and 85 wt%, there were more residues on the beaker and the surface capacity and capillary force of expanded perlite were insufficient to adsorb the excess PCM (i.e., expanded perlite had reached the saturated adsorption state under this test condition but could not adsorb all the MPCM) and the amount of perlite was relatively low at this point. When the MPCM was 75 wt% and 70 wt%, the residue was almost invisible on the beaker. The optimal adsorption of MPCM was expected to be reached at 75 wt%, the perlite dosage at 70 wt% was on the high side, and the expanded perlite did not reach saturation adsorption. The above analysis was further confirmed in Fig. 3(b), that represents the mass fraction of MPCM remaining on the beaker, from which it can be seen that MPCM at 80 wt% and 85 wt% had a relatively high residual amount of 0.55 % and 1.32 %, respectively. The residual amount of MPCM at 70 wt% and 75 wt% is 0.05 % and 0.09 %, respectively. Values that are very close to each other and may be due to the fact that MPCM had been sufficiently adsorbed, whereas it can be seen that below 75 wt%, continued adsorption was not effective and increasing the amount of perlite did not have any significant effect. For these reasons, 75 wt% of MPCM was determined as the optimum adsorption mass fraction.

Epoxy resin coating was used for leak prevention and the amount of epoxy resin required was studied by leak testing. Since the volume of expanded perlite was almost constant before and after adsorption and the overall morphology of the coating was close to the profile of expanded perlite, it was probed at the $m_{ER}:m_{EP}$ ratios = 0.4, 0.6, 0.8, 1.0, 1.2 and above. Fig. 4 shows the leakage of Coated CPCM with different epoxy resin dosage at 60 °C after holding for 1 h. From the figure, it can be seen that the uncoated CPCM showed serious leakage under long holding time, and, when the $m_{ER}:m_{EP}$ ratio was 0.4, there was no significant change in leakage, indicating that the coating can hardly form a cladding layer. With the increase of $m_{ER}:m_{EP}$, the leakage gradually improved, and when $m_{ER}:m_{EP} = 1.2$, there was almost no macroscopic visible leakage, indicating that the coating at this ratio exhibited an expected encapsulation effect and the MPCM encapsulated inside showed almost no macroscopic leakage when melted under heat. Particles at ratios above 1.2 showed more severe adhesion, indicating excessive coating. This leakage test demonstrated that epoxy encapsulation can be leak-proof and also confirmed the need for encapsulation.

3.3. Scanning electron microscope morphological analysis

Fig. 5(a)-(c) shows the microscopic morphology of EP, CPCM and Coated CPCM. It can be observed in Fig. 5(a) that expanded perlite has irregular porous structure and surface glaze layer, which, combined with the hydrophilic characteristics of expanded perlite, is conducive to the adsorption of liquid. In Fig. 5(b), the surface of the CPCM still has obvious pores, but the pores of the expanded perlite as a carrier are

significantly reduced, because the phase change material impregnated the expanded perlite and filled most of the pores. Fig. 5(c) shows the morphology of Coated CPCM. On the whole, compared with the uncoated CPCM, the surface of Coated CPCM is coated with epoxy resin. The surface is smooth and coated evenly. However, epoxy resin as a coating is mainly reflected in the surface covering layer and the plugging of small holes. For the depression and large holes, epoxy resin cannot be completely blocked. This is mainly because epoxy resin is a liquid mucus, and combined with the amount of epoxy resin, it cannot play the purpose of plugging large holes. From the coated part, the coating is uniformly covered on the outer surface, and the integrity is relatively complete.

Fig. 5(d) shows the pore size distribution curves of EP, CPCM and Coated CPCM. It can be found from this figure that the pore size range of EP is mainly 4–100 μm, the pore size range of CPCM is mainly 4–8 μm, and the pore size range of Coated CPCM is mainly 3.6–6.5 μm. The hole capacity of EP is significantly higher than that of CPCM and Coated CPCM, because the holes of the latter two are full of phase change material, and most of the holes have been blocked. The red curve also shows a distinct pore size range. This is due to the fact that the surface pores were crushed with the increase of the test pressure, indicating that the PCM could not overcome the surface tension to enter these pores. As can be seen in Fig. 5(e), the total amount of mercury injected into CPCM and Coated CPCM is far less than that on EP, which corresponds to the interpretation in Fig. 5(d). The hole is filled with phase change material. The absorption of EP makes its initial mercury intake point higher than that of CPCM and Coated CPCM. The mercury inlet on the surface of the Coated CPCM lags behind that on the CPCM. This is because the hole is further blocked by the epoxy resin. When mercury enters the hole, the corresponding hole is around 6.5 μm. This corresponds to large holes that have not been blocked by epoxy resin.

The mercury injection tests on EP, CPCM and Coated CPCM are listed in Table 3. It is found that the presence of epoxy resin has greatly reduced the porosity, and the average pore size of the composite has been reduced to 4.86 μm, with specific surface area only 0.09 m²/g. We only calculate the data above the pore size range that the phase change material can enter, which is more useful for reference.

In order to further observe and analyse the surface morphology of CPCM and Coated CPCM, scanning electron microscope is used to magnify and observe them respectively. Fig. 6(a) and (c) show the surface morphologies of CPCM at 350 times and 2000 times magnification, respectively. It can be seen that the phase change material is attached to the surface of the expanded perlite, and there are a large number of voids between each other. Although CPCM has reached the saturated adsorption state, with the increase of the number of cycles of the material, the decrease of latent heat makes its energy storage efficiency decrease. Fig. 6(b) and (d) show the surface morphologies of Coated CPCM at 350 times and 2000 times magnification respectively. It can be seen that smooth coating is on the surface of coated CPCM, which is

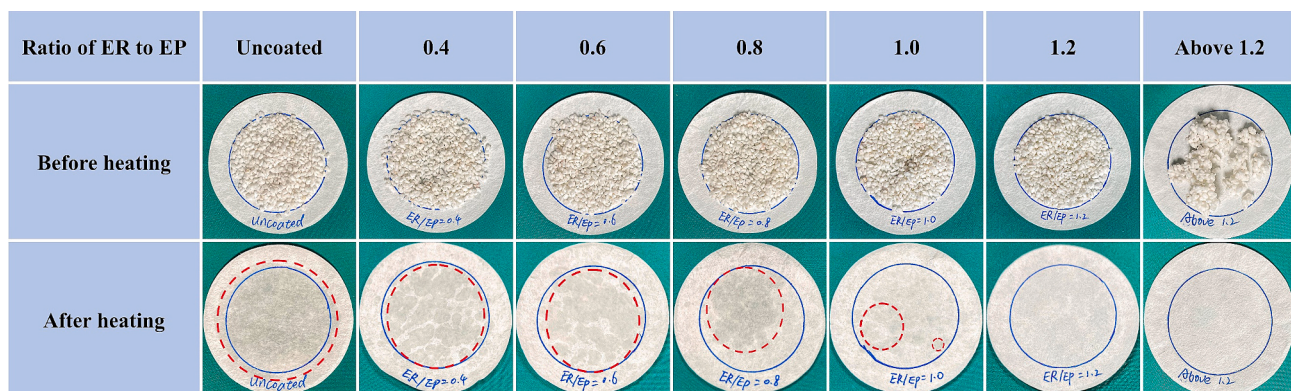


Fig. 4. The leakage test of CPCM and Coated CPCM with different epoxy resin dosage at 60 °C.

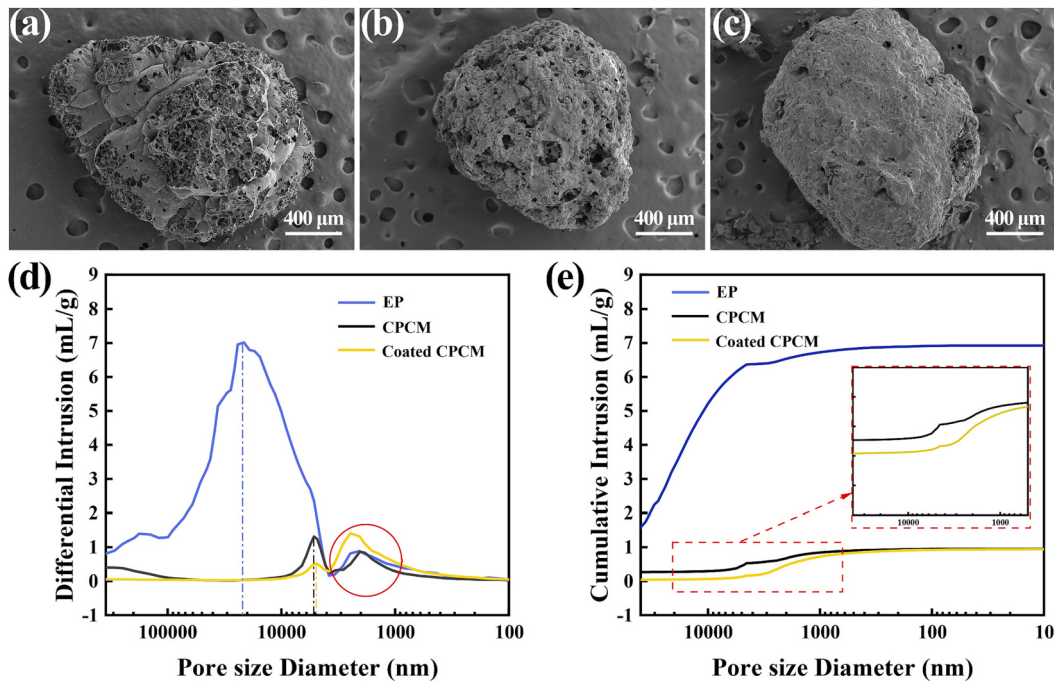


Fig. 5. SEM images of EP (a), CPCM (b) and Coated CPCM (c), pore size distribution curves of EP, CPCM and Coated CPCM (d), relationship curve between mercury injection and pore size distribution (e).

Table 3
Mercury injection test information on EP, CPCM and Coated CPCM.

Sample	Porosity ratio (%)	Average pore size (μm)	Specific surface area (m^2/g)
EP	90.36	21.33	1.54
CPCM	54.68	5.53	0.20
Coated CPCM	39.68	4.86	0.09

epoxy resin coating. The coating not only covers the expanded perlite and the exposed phase change material, but also fills some smaller holes. The existence of the coating greatly reduces the contact between phase change material and air, and to some extent alleviates the local flow of phase change material in the liquid phase state. After some saturated adsorbed particles are heated, the liquid flows to the bottom particles due to the action of gravity. As a result, the heat storage capacity of the particles accumulated on the macro level will be out of sync, which is not conducive to the overall heat storage and release.

It should be pointed out that although most epoxy resins are relatively smooth and coated completely, a small number of holes can be observed through SEM images. The reasons are mainly reflected in two aspects. First, due to the high viscosity of epoxy resins, more bubbles will be introduced in the stirring process, and the air in these bubbles cannot be eliminated in the curing process, so there are pores in the coating. The second is the bubbles produced by the curing reaction. However, the coating is sufficient to alleviate the leakage of liquid phase.

A microregion in the Coated CPCM profile was selected for EDS analysis to further investigate the elemental distribution. As shown in Fig. 6(e)-(j), the distributions of carbon, sodium, nitrogen, and oxygen elements are represented in red, purple, yellow, and green, respectively. From Fig. 6(i), it can be seen that the location with obvious sodium element distribution corresponds to the part labelled in Fig. 6(h), which indicates that the material in this part was MPCM, while the area with less element distribution may be expanded perlite and epoxy resin. After observing Fig. 6(f), (g), and (j), it can be confirmed that the area with lower element distribution was epoxy resin, because the main

components of expanded perlite are SiO_2 and Al_2O_3 , with less carbon and nitrogen elements, while epoxy resin contains more carbon, nitrogen and oxygen elements. The nitrogen elements were uniformly distributed in Fig. 6(g) (the nitrogen in MPCM was mainly derived from urea). The EDS analysis verifies and corresponds to the morphology and elemental distribution of each material in SEM. The results show that the MPCM and the coating were uniformly distributed in their respective locations.

3.4. Chemical compatibility of CPCM and coated CPCM

To investigate the chemical compatibility after adsorption and encapsulation, FT-IR tests were performed as shown in Fig. 7(a). In the characteristic spectrum of EP, the characteristic peaks of 787 cm^{-1} and 1055 cm^{-1} correspond to symmetric and asymmetric stretching vibrations of Si-O-Si, whilst 1633 cm^{-1} corresponds to water molecules producing O-H groups. In the characteristic spectrum of epoxy resin, 826 cm^{-1} and 917 cm^{-1} are the characteristic absorption peaks, typical of epoxy group. The two peaks at 1032 cm^{-1} and 1240 cm^{-1} correspond to the C=O stretching vibration of secondary alcohol and aryl ether stretching vibration respectively; finally, 1507 cm^{-1} and 1606 cm^{-1} correspond to the characteristic peaks of benzene ring.

In the characteristic spectra of MPCM, the peak close to 3370 cm^{-1} corresponds to the O-H group, indicating the presence of water, and 1406 cm^{-1} and 1546 cm^{-1} correspond to the symmetric and asymmetric stretching vibrations of C=O in the carboxyl group, respectively. The characteristic peaks in CMCM 1050 cm^{-1} , 1414 cm^{-1} , 1575 cm^{-1} , and 3431 cm^{-1} and the characteristic peaks in Coated CPCM 1049 cm^{-1} , 1414 cm^{-1} , 1571 cm^{-1} , and 3430 cm^{-1} are very close to those of the first three materials and correspond to Si-O-Si asymmetric stretching vibrations, C=O symmetric and asymmetric stretching vibrations, and O-H stretching vibrations, respectively. Some of the peak intensity decreases may be caused by surface tension due to the interaction among the materials [32]. While the synthesized materials did not produce new characteristic peaks, the spectra of CPCM and Coated CPCM were almost identical and did not show significant epoxy characteristic peaks, which was due to the volume fraction of epoxy in Coated CPCM, negligible

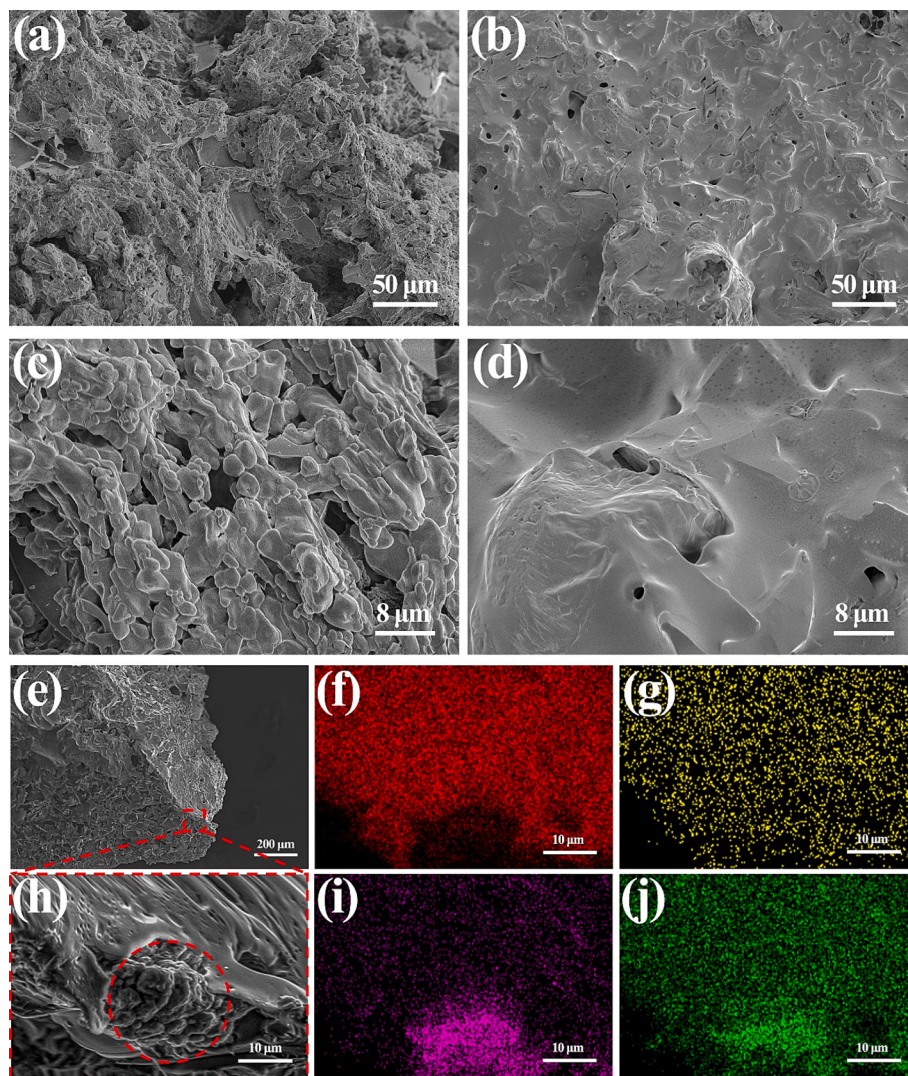


Fig. 6. SEM images of CPCM(a) \times 350, (c) \times 2000, Coated CPCM(b) \times 350, (d) \times 2000. SEM images of Coated CPCM sections (e), local enlargement (h), and EDS mapping images of corresponding elements carbon (f), sodium (i), nitrogen (g), and oxygen (j).

with respect to the lower limit of detection. These results indicate that there was no chemical reaction during the adsorption process and the coating process, but only physical interactions, indicating that the components had good chemical compatibility with each other.

To further analyse the structure of the composite material, the XRD characterization was supplemented. Fig. 7(b) is the XRD patterns of EP, ER, MPCM, CPCM and Coated CPCM. EP and ER do not show obvious diffraction peaks in their respective spectra, which indicates that both are amorphous materials. In the diffraction pattern of MPCM, $2\theta = 11.4^\circ, 12.7^\circ, 16.9^\circ, 19.1^\circ, 29.7^\circ, 33.7^\circ$ correspond to the characteristic diffraction peaks of SAT; at $2\theta = 22.2^\circ, 24.5^\circ, 29.3^\circ, 35.4^\circ, 54.8^\circ$ correspond to the characteristic peaks of urea. The position of the characteristic diffraction peak of CPCM is consistent with that of MPCM, without obvious shift, indicating that the crystal structure of MPCM and EP is good, due to the existence of EP, the diffraction intensity is slightly enhanced in the range of 0° - 50° . The spectra of Coated CPCM and CPCM are almost the same, that is, no new peaks appear after the addition of epoxy resin, indicating that the crystal structure of CPCM has not changed during the synthesis process. The epoxy resin basically did not change the crystallization state of CPCM.

FT-IR and XRD are not effective in detecting the phase with low content in composites. XPS can effectively analyse the surface elements and coordination of particles, carry out XPS test, and further analyse the

structure of composite materials to determine the bonding state of epoxy resin and CPCM. The characterization results are shown in Fig. 7(c)-(e).

The XPS survey spectrum shows that the main elements of Coated CPCM are composed of Na, C, O and so on. Among them, the C 1s peaks are located at 284.8 eV, 285.6 eV and 288.56 eV, corresponding to C=C, C—O and C≡C bonds, respectively. The O 1 s peaks are located at 531.2 eV, 532.1 eV, and 535.9 eV, corresponding to C=O, C—O and Na auger respectively, and the Na 1s peaks only appear at 1071.4 eV. It should be pointed out that C—O bonds and C=O bonds exist not only in epoxy resins, but also in sodium acetate trihydrate in CPCM. However, no new coordination state was detected in the XPS spectrum of the powder sample of Coated CPCM. Combining the SEM picture in Fig. 6(d) and FT-IR and XRD analysis, it shows that the epoxy resin is successfully attached to the surface of CPCM and they have good chemical compatibility.

3.5. Thermal stability analysis

By analysing the TG curve, we can know the composition, thermal stability, thermal decomposition of the sample and its possible intermediate products and other information related to quality. About 20 mg of MPCM, CPCM and Coated CPCM samples are heated at $10^\circ\text{C}/\text{min}$ in N_2 atmosphere. Fig. 8(a) is the physical picture of the thermal stability

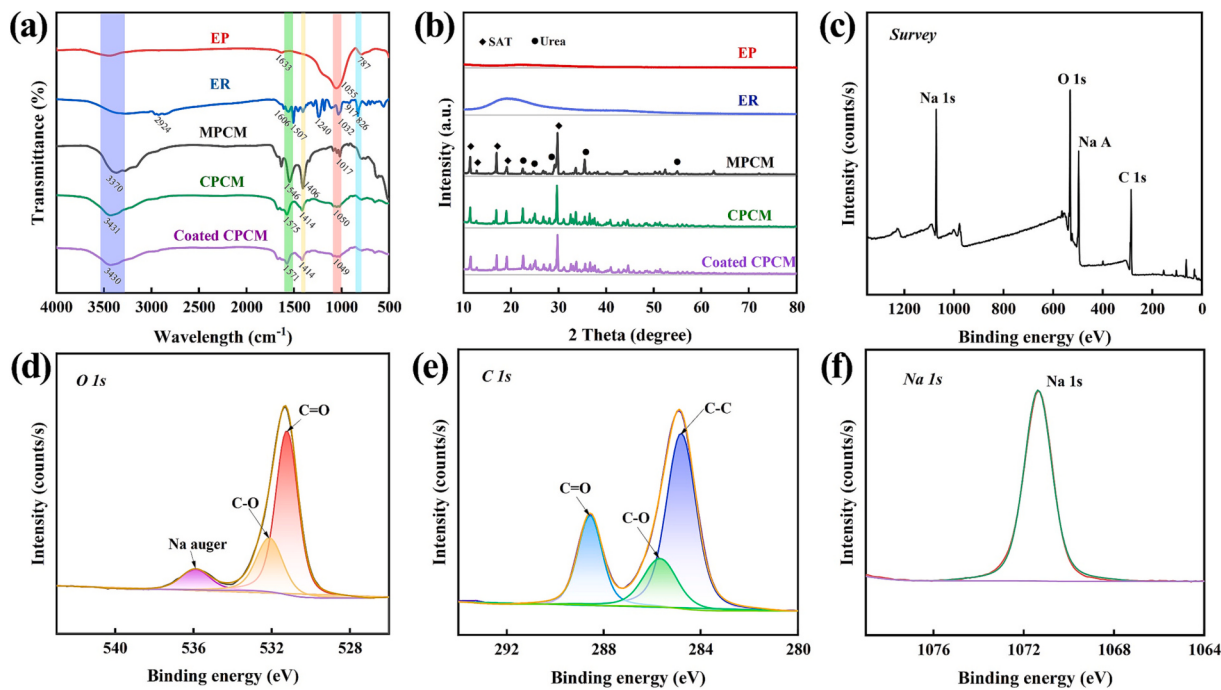


Fig. 7. FT-IR spectra (a), XRD patterns (b) of EP, ER, MPCM, CPCM, Coated CPCM, XPS survey spectra of the samples (c) and high-resolution XPS spectra in the specific binding energy ranges of O 1s (d), C 1s (e) and Na 1s (f).

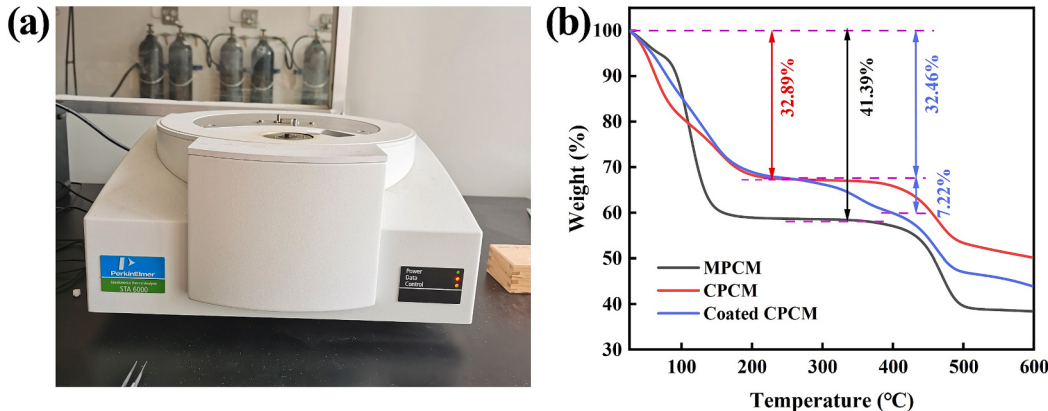


Fig. 8. (a) Equipment for thermal stability analysis, (b) Thermogravimetric curves of MPCM, CPCM, and Coated CPCM.

analysis equipment.

Fig. 8(b) shows the thermogravimetric curves of MPCM, CPCM, and Coated CPCM. For MPCM, 25–160 °C corresponds mainly to the loss of water, with a weight loss of 41.39 %, very close to the theoretical proportion of water in MPCM of 40.31 %; 400–500 °C corresponds to the decomposition of sodium acetate, and the decomposition product is sodium carbonate. For CPCM, the rate of water loss was lower than that of MPCM, mainly because the adsorption of expanded perlite, capillary force, and surface tension slowed down the evaporation of water molecules. The weight percentage of water decreased due to the introduction of expanded perlite and the actual water weight loss of 32.89 % was close to the theoretical value of 31.05 %. The error was caused by the difference in sample distribution during sampling (20 mg), the decomposition after 400 °C corresponds to the decomposition of sodium acetate, which tends to be consistent with the decomposition of MPCM. For Coated CPCM, the rate of weight loss during 25–200 °C was slower than CPCM, suggesting that the presence of the coating further inhibited the evaporation of water, and the process lost 32.46 % of the weight, including water in the hydrate and water in the coating. Since the epoxy

resin used in this experiment was aqueous and water was the continuous dispersion medium, the curing process was accompanied by the evaporation of water molecules. The water present inside was prevented from evaporation by the cured film on the surface, which indicates that film formation was also a two-phase (resin and curing agent) transforming into a single-phase process. As the temperature continued to increase, the coating partially decomposed with a weight loss of 7.22 %. As can be seen from the graph, the coating began to decompose at around 290 °C, which is sufficient for Coated CPCM working at temperatures of 60 °C and below for long periods of time.

3.6. Phase change behaviour

Fig. 9(a) shows the DSC data of pure sodium acetate trihydrate at 0 and 100 times, and compares the data with the DSC of CPCM and Coated CPCM at 0 and 100 times, as shown in Fig. 9(c). Comparing the latent heat data before and after the cycle of CPCM and Coated CPCM, it was found that the value decreased by only 6.3 % and 1.8 %, respectively, this is because the porous matrix expanded perlite impregnated

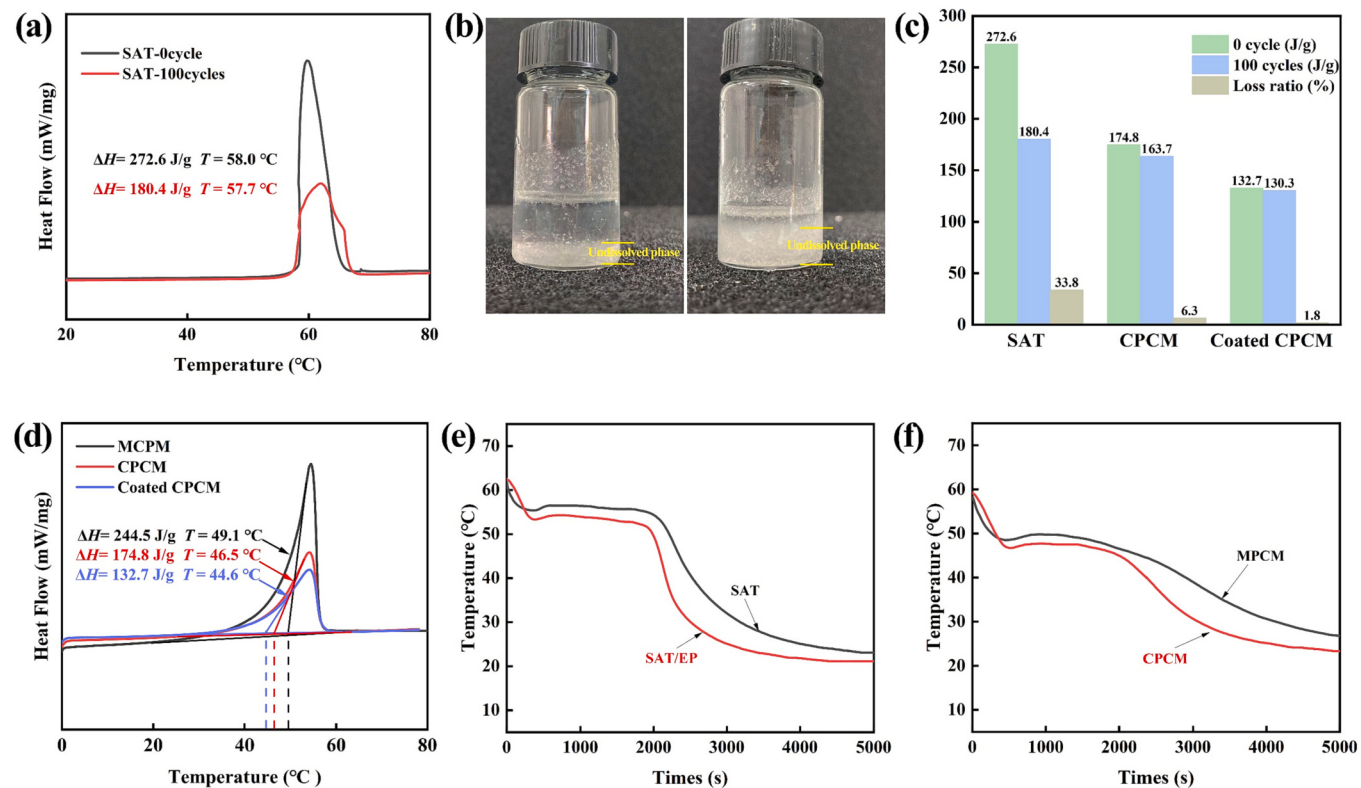


Fig. 9. DSC curves for MPCM, CPCM, and Coated CPCM.

with PCM can not only improve the problem of liquid phase leakage, but also alleviate the phenomenon of phase separation. The separation between particles makes the distribution of phase change materials more uniform and improves the service life of materials.

Suitable phase change temperatures and high latent heat of phase change are important for the application of phase change materials in buildings. The temperature of the phase change radiant heating system is between about 40–50 °C [33,34]. Although sodium acetate trihydrate has a high latent heat of phase change (271.0 J/g), its phase change temperature (58 °C) is higher than the actual heating needs, so the problem of high phase change temperature and excessive supercooling during the phase change process was solved by the preliminary modification of sodium acetate trihydrate. The DSC curve of the modified phase change material, i.e., the phase change performance of MPCM, can be seen in Fig. 9(d): the latent heat of phase change is 244.5 J/g, and the phase change temperature is 49.1 °C, which meets the heating demand. The phase change temperature of CPCM decreases compared with MPCM, from 49.1 °C to 46.5 °C, and the drop in temperature is attributed to the interaction between hydrate and porous material and the pore confinement effect. The strong surface interaction between the phase change material and the carrier causes an increase in the temperature of the phase change material within the void, while the weak surface interaction decreases the phase change temperature [35,36], as observed in Fig. 6(a), the interaction forces between MPCM and EP were surface tension and capillary forces, which were weak and thus led to a decrease in the phase change temperature.

The variation of the latent heat of phase change of CPCM can be calculated by Eq. (1)

$$\Delta H_{CPCM} = \Delta H_{MPCM} \cdot \frac{m_{MPCM}}{m_{MPCM} + m_{EP}} \quad (1)$$

where ΔH is the latent heat of phase change, and m is the mass. It is calculated that the theoretical latent heat of phase change of CPCM is 183.5 J/g, and the actual latent heat of phase change is 174.8 J/g, which

was 95.3 % of the theoretical value, and the testing error and adsorption inhomogeneity will lead to the error between the actual value and the theoretical value. The error is within the acceptable range in this case.

Similarly, the variation of the latent heat of phase change for Coated CPCM can still be calculated using Eq. (1). The theoretical latent heat of phase change for Coated CPCM is 134.5 J/g and the actual latent heat of phase change is 132.7 J/g, which is 98.7 % of the theoretical value. As the percentage of MPCM in the total mass keeps decreasing, the latent heat also decreases. Compared with CPCM, the latent heat of Coated CPCM decreased by 42.1 J/g. However, the volume proportion of epoxy resin in Coated CPCM was small and did not significantly change the volume unit MPCM mass, so its energy storage density should be close to that of CPCM. In terms of phase change temperature, 44.6 °C of Coated CPCM is close to 46.5 °C of CPCM, and despite the decrease, this temperature still satisfies the phase change radiant heating system.

Comparing the phase transition temperature changes of SAT (10.00 g), modified SAT (10.00 g) and expanded perlite in the same proportion before and after mixing, it can be seen from Fig. 9(e) that the actual phase transition temperature of pure SAT is 56.5 °C, the actual phase change of SAT/EP is 54.3 °C, and the temperature change is 2.2 °C. The modified SAT, that is, MPCM, has an actual phase transition temperature of 49.7 °C, and CPCM has an actual phase transition temperature of 47.7 °C, with a temperature change of 2.0 °C, as shown in Fig. 9(f). That is to say, the expanded perlite at this ratio, mainly due to its pore effect, has basically the same effect on the phase transition temperature of the PCM, ranging from 2.0 °C to 2.2 °C, which is close to the test result of 2.6 °C (49.1 °C dropped to 46.5 °C, the data obtained by DSC).

3.7. Thermal reliability and applications

The phase change temperature and the latent heat of phase change of the material after multiple heating-cooling cycle processes are a measure of thermal reliability. To investigate the protection of the coating against latent heat, DSC tests were performed on samples before and

after cycling of CPCM and Coated CPCM to investigate the latent heat loss of both. As can be seen in Fig. 10(a), after 100 cycles of testing, the latent heat of phase change of CPCM decreased from 174.8 J/g to 163.7 J/g, a 6.3 % decrease, and that of Coated CPCM decreased from 132.7 J/g to 130.3 J/g, a 1.8 % decrease. This indicates that the presence of the coating has a suppressive effect on the reduction of the latent heat. Although the expanded perlite has good adsorption capacity, after a certain cycle, the liquid phase in the MPCM adsorbed on its surface

escapes more, resulting in a large latent heat loss. In contrast, the protective effect of the coating makes the escape rate of the liquid phase in MPCM lower, which in turn allows the phase change material to work with a higher heat storage and discharge efficiency, which is beneficial to the long-term use and maintenance cost of the phase change radiant heating system.

Whether the phase change material can maintain a relatively constant heat dissipation temperature and small supercooling during the

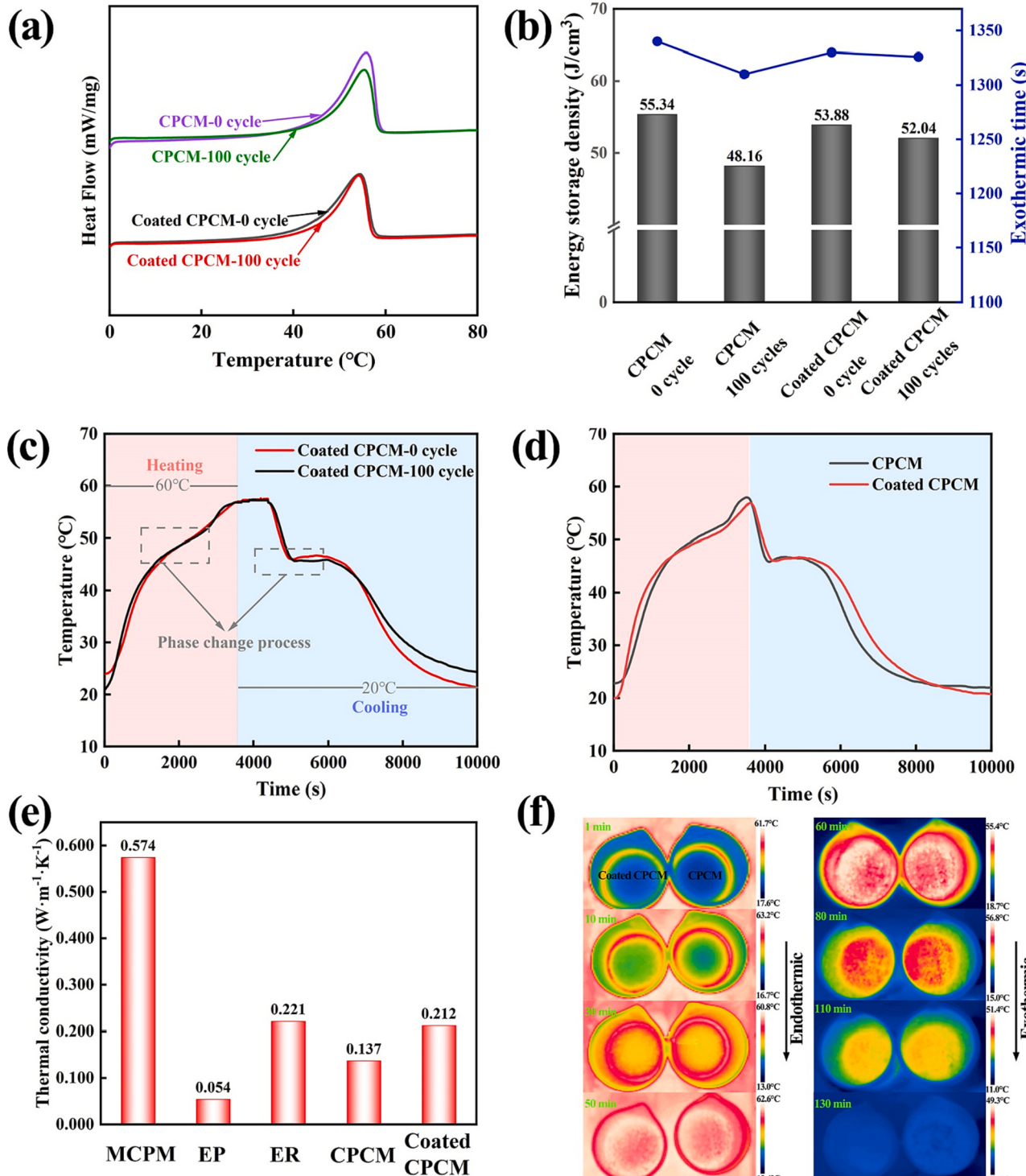


Fig. 10. (a) DSC curves, (b) energy storage density of 0 and 100 cycles of CPCM and Coated CPCM, (c) Step cooling curves of 0 and 100 cycles of Coated CPCM, (d) Step cooling curves of CPCM and Coated CPCM, (e) thermal conductivity of MPCM, EP, ER, CPCM and Coated CPCM in the heating and cooling processes, (f) Infrared thermal image photos of CPCM and Coated CPCM in the heating and cooling processes.

phase change process is another important concern in its practical application. Differential scanning calorimetry tests differ from the actual thermal behaviour of the material during cooling, e.g., the DSC curve does not accurately reflect the actual supercooling of the sample. Fig. 10(c) gives the heating-cooling curves of Coated CPCM before and after 100 cycles, and it can be seen that the thermal behaviour of the material after cycling is almost the same as that without cycling, and the difference in room temperature affects the difference between the two in the heat dissipation process. It should be noted that the actual phase change temperatures of CPCM and Coated CPCM were higher than the phase change temperatures in the DSC curves in several tests, which may be due to the low heat transfer efficiency of the materials affecting the temperature transfer in the actual measurements, making the thermocouple measurements slightly higher than the theoretical exothermic temperature.

The volume energy storage density of CPCM and Coated CPCM has been calculated, as shown in Fig. 10(b). Compared with the variation of DSC, this data is more valuable for reference. The volume density of the uncycled CPCM is 55.34 J/cm^3 , slightly higher than the 53.88 J/cm^3 Coated CPCM. In other words, there is not much difference between the energy density per unit volume of the two materials. This is because the epoxy resin coated on the surface of the particle has very little influence on the overall volume of the material. The change of mass should be considered in DSC calculation. After 100 cycles, the volume density of the Coated CPCM has dropped to 48.16 J/cm^3 , while the Coated CPCM only drops to 52.04 J/cm^3 . The reduction in volume density makes it possible to maintain the energy storage and release efficiency during the cycle. The latent heat release time of the two samples before and after the cycle has been calculated. The heat release time of the Coated CPCM is almost the same as that before the cycle.

Fig. 10(e) shows the thermal conductivity of the expanded perlite EP, ER, CPCM and Coated CPCM. As a kind of thermal insulation material, expanded perlite has a low thermal conductivity of 0.054 W/(mK) , making the thermal conductivity of CPCM only 0.137 W/(mK) . The thermal conductivity of Coated CPCM is 0.212 W/(mK) , higher than that of the CPCM, 0.137 W/(mK) . This is because the epoxy resin is attached to the surface of the CPCM, and the heat transfer is mainly through the particles on the epoxy resin in contact with each other. Therefore, the thermal conductivity of the Coated CPCM is close to that of the epoxy resin. It can be said that the existence of the epoxy resin enhances the heat transfer rate of the CPCM. In addition, in a broad sense, PCM with low thermal conductivity is considered to be an excellent indoor insulation material, allowing for slow and prolonged heat release.

The curves of heating (60°C)–cooling (20°C) of CPCM and Coated CPCM with the same volume are provided, as shown in Fig. 10(d). It can be seen that the heating rate of Coated CPCM is slightly higher than that of CPCM, but the difference is small. This shows that in the actual heat transfer process, the effect of epoxy resin on heat conduction is not obvious.

The image of the transient temperature distribution of CPCM and Coated CPCM during the heating process has been supplemented with the infrared thermal image recorder (experimental conditions are in accordance with Fig. 10(f)). Different colours represent the corresponding temperature, the ambient temperature of the base colour. The temperature of the material near the container wall is always higher than that of the material in the middle, which is determined by the low thermal conductivity of the material. The temperature rise of Coated CPCM is slightly faster than that of Coated CPCM. Combined with the thermal conductivity of the material coated CPCM in Fig. 10(e), it can be seen that this is because of the high thermal conductivity of the coated CPCM. However, as the thermal conductivity of the two materials is relatively low, there is no obvious difference in the infrared image. The material approaches the heating temperature at 3000 s , which corresponds to the heating time of the material in Fig. 10(d). After the heating is stopped, it is cooled at room temperature. After 4200 s , it drops to room temperature, which indicates that the material has a long heat

release time, long insulation effect and good heat storage capacity.

The specific phase change properties for 0 and 100 cycles of CPCM, Coated CPCM data are listed with Table 4.

The thermal management properties of the material were investigated. Fig. 11(a) shows the model drawing of the homemade thermal chamber, a space with dimensions of $300 \text{ mm} \times 300 \text{ mm} \times 300 \text{ mm}$ was constructed with 2-mm-thick wood plywood and 40-mm-thick polystyrene foam insulation board was pasted on the inside of the bottom plywood. The phase change material board was located on top of the insulation board, and to release the temperature in a comfortable range, a layer of polystyrene board was placed on top of the phase change material board. The insulation box was moved from a room temperature of 25°C to an environment of 8°C , and the time required to reduce the internal temperature of the insulation box to 8°C was recorded, and the improvement of the insulation box temperature by the phase change material board with thicknesses of 5 mm, 10 mm, and 15 mm were tested. The results are shown in Fig. 11(b). It can be seen that the thermal chamber without phase change material dropped to the ambient temperature in only 1.09 h. In comparison, the delay in temperature reduction was significant for the phase change material plates, with 4.05 h, 5.04 h, and 6.52 h for the 5 mm, 10 mm, and 15 mm plates, respectively, which was attributed to the excellent thermal storage capacity of the phase change material, and therefore can exhibit long-lasting thermal management performance. In conclusion Coated CPCM has a good potential as a promising thermal energy storage material for radiant floor heating applications.

4. Conclusion

In this paper, Coated CPCM with sodium acetate trihydrate as the main heat storage medium, expanded perlite as the adsorption carrier and epoxy resin as the dense coating were successfully prepared. The adsorption of MPCM by different mass percentages of expanded perlite and the effect of different amounts of coating on leakage prevention were investigated. The main results are the followings.

- (1) In the preparation of CPCM, the optimal adsorption ratio of MPCM was found to be 75 wt%, at which the expanded perlite just reached the saturated adsorption state. The optimal $m_{\text{ER}}:m_{\text{EP}}$ ratio in Coated CPCM was 1.2, at which the coating can guarantee complete encapsulation, while avoiding the adhesion between the particles, also resulting in a better effect in stopping the leakage of liquid phase.
- (2) Adsorption and encapsulation processes, with good chemical compatibility between the components. The mechanism that has influence on the reduction of the phase change temperature was mainly weak interaction forces, such as surface tension and capillary forces, and the reduction of latent heat was mainly attributed to the introduction of expanded perlite and epoxy resin, which reduced the mass share of MPCM. The experimental data were very close to the theoretical ones in phase change and the errors were due to the preparation and testing process.
- (3) The thermal reliability analysis shows that due to the protective effect of the coating, the escape of moisture from Coated CPCM was slowed down, and the efficiency of recycling was improved.

Table 4
Phase change properties of CPCM, Coated CPCM for 0 and 100 cycles.

		$\Delta H_{\text{DSC}}(\text{J/g})$	$T_{\text{DSC}}(\text{ }^\circ\text{C})$	$T_{\text{Step cooling}}(\text{ }^\circ\text{C})$	$\Delta T_{\text{Step cooling}}(\text{ }^\circ\text{C})$
CPCM	0 cycle	174.8	46.5	47.7	0.6
	100 cycles	163.7	46.1	47.3	1.0
Coated CPCM	0 cycle	132.7	44.6	46.4	0.6
	100 cycles	130.3	44.3	45.8	0.3

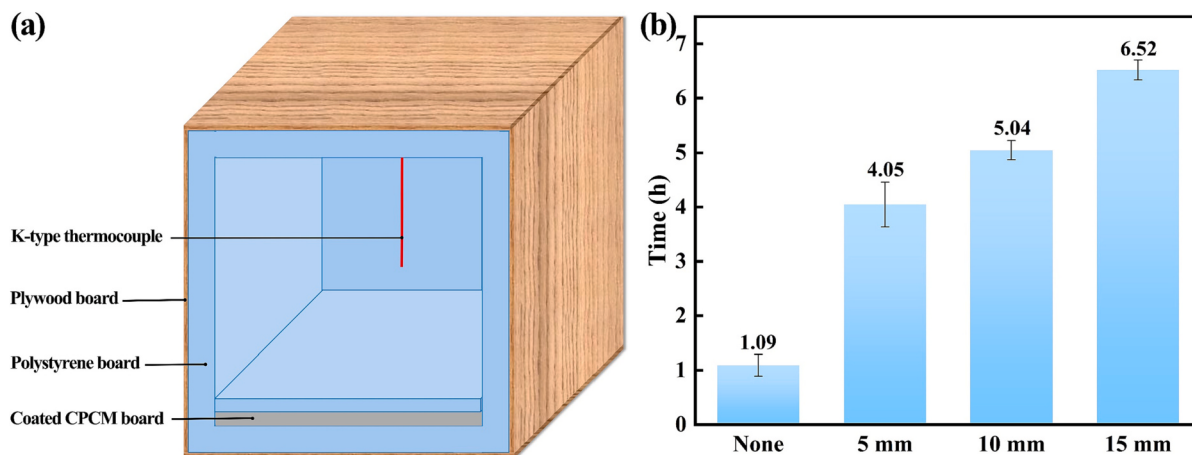


Fig. 11. (a) Schematic diagram of insulation box, (b) Insulation effect of Coated CPCM panels on the insulation box.

The latent heat of phase change of Coated CPCM was 132.7 J/g, the actual phase change temperature was 46.4 °C, and the supercooling temperature is 0.6 °C. After 100 cycles, the latent heat of phase change dropped to 130.3 J/g, the drop was only 1.8 %, and the phase change temperature did not change significantly, with good thermal reliability.

- (4) Insulated boxes containing Coated CPCM had a significant delayed temperature reduction effect and exhibit longer lasting thermal management performance.

In conclusion, Coated CPCM resulted in having a greater prospect for application in radiant floor insulation systems having high latent heat, suitable phase change temperature, and excellent thermal cycle stability. However, this study did not solve the problem of porosity generated by the curing process of epoxy resin, and conducted a full modification study. In the later work, there should be further research on how to reduce the porosity generated by the curing process of epoxy resin.

CRediT authorship contribution statement

Henghua Zhang: Conceptualization, Formal analysis, Investigation, Methodology, Writing – original draft. **Qianbin Dong:** Data curation, Formal analysis. **Juetian Lu:** Investigation, Formal analysis. **Yaping Tang:** Supervision, Writing – review & editing. **Wenjian Bi:** Project administration, Writing – review & editing. **Yue Gao:** Investigation, Writing – review & editing. **Hui Yang:** Conceptualization, Supervision, Validation, Writing – review & editing. **Jiabang Wang:** Funding acquisition, Supervision.

Declaration of competing interest

The authors declare the following financial interests/personal relationships which may be considered as potential competing interests: Yaping Tang, Wenjian Bi, Yue Gao report equipment, drugs, or supplies and statistical analysis were provided by Zhejiang Kesheng Technology Co., LTD.

Data availability

Data will be made available on request.

Acknowledgements

I would like to express my sincere gratitude to my tutor, senior students and other experimenters for their guidance and help in completing this work. The authors also thank Shiyanjia Lab (www.shiyanjia.com)

for the FT-IR test as well as SEM by Mrs. Zheng Na and DSC by Mrs. Xu Li from State Key Laboratory of Chemical Engineering in Zhejiang University.

References

- [1] N. Xie, J. Luo, Z. Li, Z. Huang, X. Gao, Y. Fang, Salt hydrate/expanded vermiculite composite as a form-stable phase change material for building energy storage, *Sol. Energy Mater. Sol. Cells* 189 (2019) 33–42, <https://doi.org/10.1016/j.solmat.2018.09.016>.
- [2] V.S.K.V. Harish, A. Kumar, A review on modeling and simulation of building energy systems, *Renew. Sust. Energ. Rev.* 56 (2016) 1272–1292, <https://doi.org/10.1016/j.rser.2015.12.040>.
- [3] M. Izquierdo, P. de Agustin-Camacho, Solar heating by radiant floor: experimental results and emission reduction obtained with a micro photovoltaic-heat pump system, *Appl. Energy* 147 (2015) 297–307, <https://doi.org/10.1016/j.apenergy.2015.03.007>.
- [4] N. Xie, X.N. Gao, Y. Zhong, R.D. Ye, S. Chen, L.X. Ding, T. Zhong, Enhanced thermal performance of Na₂HPO₄ 12H₂O composite phase change material supported by sepiolite fiber for floor radiant heating system, *J. Build. Eng.* 56 (2022), 104747, <https://doi.org/10.1016/j.jobe.2022.104747>.
- [5] M. Song, F. Niu, N. Mao, Y. Hu, S. Deng, Review on building energy performance improvement using phase change materials, *Energy Build.* 158 (2018) 776–793, <https://doi.org/10.1016/j.enbuild.2017.10.066>.
- [6] R. Barzin, J.J.J. Chen, B.R. Young, M.M. Farid, Application of PCM underfloor heating in combination with PCM wallboards for space heating using price based control system, *Appl. Energy* 148 (2015) 39–48, <https://doi.org/10.1016/j.apenergy.2015.03.027>.
- [7] M. Li, Z. Wu, H. Kao, J. Tan, Experimental investigation of preparation and thermal performances of paraffin/bentonite composite phase change material, *Energy Convers. Manag.* 52 (2011) 3275–3281, <https://doi.org/10.1016/j.enconman.2011.05.015>.
- [8] H. He, P. Zhao, Q. Yue, B. Gao, D. Yue, Q. Li, A novel polynary fatty acid/sludge ceramsite composite phase change materials and its applications in building energy conservation, *Renew. Energy* 76 (2015) 45–52, <https://doi.org/10.1016/j.renene.2014.11.001>.
- [9] J. Zuo, W. Li, L. Weng, Thermal properties of lauric acid/1-tetradecanol binary system for energy storage, *Appl. Therm. Eng.* 31 (2011) 1352–1355, <https://doi.org/10.1016/j.applthermaleng.2011.01.008>.
- [10] M.M. Farid, A.M. Khudhair, S.A.K. Razack, S. Al-Hallaj, A review on phase change energy storage: materials and applications, *Energy Convers. Manag.* 45 (2004) 1597–1615, <https://doi.org/10.1016/j.enconman.2003.09.015>.
- [11] M.K. Rathod, J. Banerjee, Thermal stability of phase change materials used in latent heat energy storage systems: a review, *Renew. Sust. Energ. Rev.* 18 (2013) 246–258, <https://doi.org/10.1016/j.rser.2012.10.022>.
- [12] G.C. Sang, H.N. Zeng, Z.Q. Guo, H.Z. Cui, Y.K. Zhang, X.L. Cui, L. Zhang, W. Han, Studies of eutectic hydrated salt/polymer hydrogel composite as form-stable phase change material for building thermal energy storage, *J. Build. Eng.* 59 (2022), 105010, <https://doi.org/10.1016/j.jobe.2022.105010>.
- [13] Z. Khan, Z. Khan, A. Ghafoor, A review of performance enhancement of PCM based latent heat storage system within the context of materials, thermal stability and compatibility, *Energy Convers. Manag.* 115 (2016) 132–158, <https://doi.org/10.1016/j.enconman.2016.02.045>.
- [14] W.G. Su, J. Darkwa, G. Kokogiannakis, Review of solid-liquid phase change materials and their encapsulation technologies, *Renew. Sust. Energ. Rev.* 48 (2015) 373–391, <https://doi.org/10.1016/j.rser.2015.04.044>.
- [15] G.H. Ye, G.Q. Zhang, L.Q. Jiang, X.Q. Yang, Temperature control of battery modules through composite phase change materials with dual operating

- temperature regions, *Chem. Eng. J.* 449 (2022), 137733, <https://doi.org/10.1016/j.cej.2022.137733>.
- [16] D.Y. Niu, Y.F. Tan, T.T. Zhang, X.D. Zhang, W.S. Zhang, Thermal properties and application of a novel $\text{CaCl}_2 \cdot 6\text{H}_2\text{O}$ /expanded graphite shape-stabilized composite phase change material for electric radiant heating, *J. Energy Storage* 55 (2022), 105458, <https://doi.org/10.1016/j.est.2022.105458>.
- [17] Y.D. Bian, K.J. Wang, J.L. Wang, Y.S. Yu, M.Y. Liu, Y.J. Lv, Preparation and properties of capric acid: stearic acid/hydrophobic expanded perlite-aerogel composite phase change materials, *Renew. Energy* 179 (2021) 1027–1035, <https://doi.org/10.1016/j.renene.2021.07.125>.
- [18] M. Li, J.B. Shi, Mechanical and thermal performance assessment of paraffin/expanded vermiculite-diatomite composite phase change materials integrated mortar: experimental and numerical approach, *Sol. Energy* 227 (2021) 343–353, <https://doi.org/10.1016/j.solener.2021.09.014>.
- [19] H.Y. Wu, R.T. Chen, Y.W. Shao, X.D. Qi, J.H. Yang, Y. Wang, Novel flexible phase change materials with mussel-inspired modification of melamine foam for simultaneous light-actuated shape memory and light-to-thermal energy storage capability, *ACS Sustain. Chem. Eng.* 7 (2019) 13532–13542, <https://doi.org/10.1021/acssuschemeng.9b03169>.
- [20] Z.J. Mo, P.J. Mo, M.M. Yi, Z.Y. Hu, G.Z. Tan, M.S. Selim, Y. Chen, X. Chen, Z. Hao, X. Wei, $\text{Ti}^{3+}\text{C}^{2+}\text{Tx}$ @Polyvinyl alcohol foam-supported phase change materials with simultaneous enhanced thermal conductivity and solar-thermal conversion performance, *Sol. Energy Mater. Sol. Cells* 219 (2021), 110813, <https://doi.org/10.1016/j.solmat.2020.110813>.
- [21] V. Chinnasamy, J. Heo, S.Y. Jung, H.S. Lee, H.H.Y. Cho, Shape stabilized phase change materials based on different support structures for thermal energy storage applications-a review, *Energy* 262 (2023), 125463, <https://doi.org/10.1016/j.energy.2022.125463>.
- [22] I. Baskar, M. Chellappandian, S.S.H. Jaswanth, Development of a novel composite phase change material based paints and mortar for energy storage applications in buildings, *J. Energy Storage* 55 (2022), 105829, <https://doi.org/10.1016/j.est.2022.105829>.
- [23] Z. Rao, T. Xu, C. Liu, Z. Zheng, L. Liang, K. Hong, Experimental study on thermal properties and thermal performance of eutectic hydrated salts/expanded perlite form-stable phase change materials for passive solar energy utilization, *Sol. Energy Mater. Sol. Cells* 188 (2018) 6–17, <https://doi.org/10.1016/j.solmat.2018.08.012>.
- [24] R. Ye, C. Zhang, W. Sun, X. Fang, Z. Zhang, Novel wall panels containing $\text{CaCl}_2 \cdot 6\text{H}_2\text{O}-\text{Mg}(\text{NO}_3)_2 \cdot 6\text{H}_2\text{O}$ /expanded graphite composites with different phase change temperatures for building energy savings, *Energy Build.* 176 (2018) 407–417, <https://doi.org/10.1016/j.enbuild.2018.07.045>.
- [25] R. Huang, J. Feng, Z. Ling, X. Fang, Z. Zhang, A sodium acetate trihydrate-formamide/expanded perlite composite with high latent heat and suitable phase change temperatures for use in building roofs, *Constr. Build. Mater.* 226 (2019) 859–867, <https://doi.org/10.1016/j.conbuildmat.2019.07.331>.
- [26] V.V. Tyagi, S.C. Kaushik, S.K. Tyagi, T. Akiyama, Development of phase change materials based microencapsulated technology for buildings: a review, *Renew. Sust. Energ. Rev.* 15 (2011) 1373–1391, <https://doi.org/10.1016/j.rser.2010.10.006>.
- [27] M.M. Umair, Y. Zhang, K. Iqbal, S. Zhang, B. Tang, Novel strategies and supporting materials applied to shape-stabilize organic phase change materials for thermal energy storage-a review, *Appl. Energy* 235 (2019) 846–873, <https://doi.org/10.1016/j.apenergy.2018.11.017>.
- [28] P. Cheng, K. Wei, W. Shi, J. Shi, S. Wang, B. Ma, Preparation and performance analysis of phase change microcapsule/epoxy resin composite phase change material, *J. Energy Storage* 47 (2022), 103581, <https://doi.org/10.1016/j.est.2021.103581>.
- [29] X. Wang, Y. Gao, N. Han, X. Zhang, W. Li, Design and synthesis of microcapsules with cross-linking network supporting core for supercooling degree regulation, *Energy Build.* 253 (2021), 111437, <https://doi.org/10.1016/j.enbuild.2021.111437>.
- [30] Z. Tao, H. Wang, J. Liu, W. Zhao, Z. Liu, Q. Guo, Dual-level packaged phase change materials - thermal conductivity and mechanical properties, *Sol. Energy Mater. Sol. Cells* 169 (2017) 222–225, <https://doi.org/10.1016/j.solmat.2017.05.030>.
- [31] K. Yuan, Y. Zhou, W. Sun, X. Fang, Z. Zhang, A polymer-coated calcium chloride hexahydrate/expanded graphite composite phase change material with enhanced thermal reliability and good applicability, *Compos. Sci. Technol.* 156 (2018) 78–86, <https://doi.org/10.1016/j.compscitech.2017.12.021>.
- [32] N. Xie, J. Niu, Y. Zhong, X. Gao, Z. Zhang, Y. Fang, Development of polyurethane acrylate coated salt hydrate/diatomite form-stable phase change material with enhanced thermal stability for building energy storage, *Constr. Build. Mater.* 259 (2020), 119714, <https://doi.org/10.1016/j.conbuildmat.2020.119714>.
- [33] M. Li, Z. Lin, Y. Sun, F. Wu, T. Xu, H. Wu, X. Zhou, D. Wang, Y. Liu, Preparation and characterizations of a novel temperature-tuned phase change material based on sodium acetate trihydrate for improved performance of heat pump systems, *Renew. Energy* 157 (2020) 670–677, <https://doi.org/10.1016/j.renene.2020.05.061>.
- [34] X. Jin, F. Wu, T. Xu, G. Huang, H. Wu, X. Zhou, D. Wang, Y. Liu, A.C.K. Lai, Experimental investigation of the novel melting point modified phase-change material for heat pump latent heat thermal energy storage application, *Energy* 216 (2021), 119191, <https://doi.org/10.1016/j.energy.2020.119191>.
- [35] D. Zhang, S. Tian, D. Xiao, Experimental study on the phase change behavior of phase change material confined in pores, *Sol. Energy* 81 (2007) 653–660, <https://doi.org/10.1016/j.solener.2006.08.010>.
- [36] J.F. Rodrigues, J.M. Urbano, On a Darcy-Stefan problem arising in freezing and thawing of saturated porous media, *Contin. Mech. Thermodyn.* 11 (1999) 181–191, <https://doi.org/10.1007/s001610050110>.